

# FSAG: Enhancing Human-to-Dexterous-Hand Finger-Specific Affordance Grounding via Diffusion Models

Yifan Han<sup>1,2</sup>, Yichuan Peng<sup>5</sup>, Pengfei Yi<sup>1,2</sup>, Junyan Li<sup>1,2</sup>, Hanqing Wang<sup>3</sup>,  
Gaojing Zhang<sup>4</sup>, Qi Peng Liu<sup>5</sup>, Wenzhao Lian<sup>5†</sup>



Fig. 1. **Overview.** FSAG learns finger-specific affordance fields from human demonstrations by leveraging semantic priors of hand-object interactions from a frozen Stable Diffusion model [1]. by conditioning grasp synthesis on affordance field learned from human demonstrations, our method generates human-intuitive and physically stable grasps, without requiring any robot action data.

**Abstract**—Dexterous grasp synthesis must jointly satisfy functional intent and physical feasibility, yet existing pipelines often decouple semantic grounding from refinement, yielding unstable or non-functional contacts under object and pose variations. This challenge is exacerbated by the high dimensionality and kinematic diversity of multi-fingered hands, which makes many methods rely on large, hardware-specific grasp datasets collected in simulation or through costly real-world trials. We propose a data-efficient framework that bypasses robot grasp data collection by exploiting object-centric semantic priors in pretrained generative diffusion models. Temporally aligned and fine-grained grasp affordances are extracted from raw human video demonstrations and fused with 3D scene geometry from depth images to infer semantically grounded contact targets. We further incorporate these affordance regions into the grasp refinement objective, explicitly guiding each fingertip toward its predicted region during optimization. The resulting system produces stable, human-intuitive multi-contact grasps across common objects and tools, while exhibiting strong generalization to previously unseen object instances within a category, pose variations, and multiple hand embodiments. This work (i) introduces a semantic affordance extraction pipeline leveraging vision–language generative priors for dexterous grasping, (ii) demonstrates cross-hand generalization without constructing hardware-specific grasp datasets, and (iii) establishes that a single depth modality suffices for high-performance grasp synthesis when coupled with foundation-model semantics. Our results highlight a path toward scalable, hardware-agnostic dexterous manipulation driven by human demonstrations and pretrained generative models.

## I. INTRODUCTION

Reliable grasp synthesis remains a central, yet unresolved, challenge in dexterous robot manipulation. Compared with parallel-jaw grippers, multi-fingered dexterous hands offer

substantially higher kinematic expressivity and potential contact richness, but this increase in dimensionality and hand–object–environment interaction complexity dramatically amplifies the difficulty of learning and deploying robust grasp strategies. The classical problem can be informally factorized into (i) “*how to grasp*”: the structured, role-aware coordination of fingers, contacts, approach direction, and hand synergies, and (ii) “*where to grasp*”: the spatial localization of functionally exploitable object regions. Despite rapid progress, existing methods typically address these two issues in isolation, leading to brittle policies, embodiment entanglement, and limited cross-object generalization.

On “*how to grasp*”, recent works leverage reinforcement learning or large-scale supervised training in simulation to explore expansive action spaces [2], [3]. However, simulation-trained policies customarily rely on privileged, complete, and noise-free geometric states, which are rarely attainable in real-world deployments. This induces significant sim-to-real gaps when facing realistic sensing artifacts such as partial views, self-occlusions, depth discontinuities, and modality noise. An alternative line—direct large-scale real-world data collection (e.g., AnyDexGrasp [4])—suffers from prohibitive operational cost and still struggles to generalize to unseen dexterous hand embodiments. A core culprit is representational overfitting: action/policy parameterizations are tightly coupled to a specific hand model’s joint layout, contact affordances, and actuation limits, precluding systematic transfer.

On “*where to grasp*”, prevailing affordance research yields coarse region-of-interest predictions [5], [6]. While such representations offer a spatial prior for potential contact regions, they stop short of encoding the per-finger engagement strategy and the geometry-conditioned sequencing necessary for stable multi-contact closure. Thus, although they identify candidate regions, they fail to specify the fine-grained per-finger instructions required for dexterous manipulation (e.g.,

<sup>1</sup>Institute of Automation, Chinese Academy of Sciences.; <sup>2</sup>School of Artificial Intelligence, University of Chinese Academy of Sciences.; <sup>3</sup>The Hong Kong University of Science and Technology (Guangzhou).; <sup>4</sup>University of Sussex.; <sup>5</sup>School of Artificial Intelligence, Shanghai Jiao Tong University. lianwenzhao@sjtu.edu.cn.; <sup>†</sup>Corresponding Author.

contact assignments, approach vectors, and local-geometry adaptations). Recasting contact reasoning as keypoint detection is likewise insufficient: reliable contact loci often lack discriminative RGB cues and hinge on object-part semantics and inter-finger relations that appearance-only backbones (e.g., CNNs/ViTs [7]) do not capture.

Our core idea to tackle the above challenges is that Internet-scale text-to-image diffusion models internalize multi-level knowledge about objects, parts, materials, and functional geometry [1]. Prior work [8] shows that intermediate denoising features encode exactly the semantic priors missing in standard discriminative backbones, and that these features can be repurposed—not to generate data, but to ground grasp semantics.

Building on this insight, we infer a *Finger-Specific Affordance Field (FSAF)* that unifies the “where” and “how” of dexterous contacts: an object-conditioned field that assigns each surface location a finger-conditioned likelihood and role descriptor, capturing feasible contact placement and inter-finger compatibility. We repurpose a frozen Stable Diffusion [1] U-Net as a semantic backbone to predict FSAF from image–text inputs, and integrate it into an optimization-based grasp refinement and execution pipeline. Given the inferred FSAF, we synthesize finger-consistent grasps without additional teleoperation by warm-starting refinement toward the predicted regions, and transfer across heterogeneous dexterous hands by changing only the kinematic model (no retraining). Experiments show strong generalization to seen and unseen objects, improved affordance grounding, and high real-robot grasp success with cross-embodiment transfer.

In summary, we make the following contributions:

- **Finger-Specific Affordance Field (FSAF).** We introduce a fine-grained, per-finger affordance representation that leverages vision–language generative priors to jointly encode object affordance functions and contact-level manipulation semantics, decomposing monolithic grasp poses into semantically grounded finger role assignments.
- **Demonstration-light, affordance-conditioned grasp synthesis.** Our grasp generation consumes the inferred FSAF to synthesize stable, role-constrained multi-finger grasp configurations without requiring large-scale teleoperation demonstration corpora, substantially reducing data collection burden.
- **Cross-embodiment generalization.** We achieve direct transfer of grasp strategies across heterogeneous dexterous hands, evidencing that the proposed affordance abstraction disentangles grasp semantics from specific embodiment kinematics.

## II. RELATED WORK

### A. Learning from Human Demonstration Videos

Learning from human demonstration videos is central to robot learning because such data are easier to collect and encode strong task priors [6], [9]; however, a persistent embodiment gap separates human hands from robotic dexterous end-effectors. The prevailing remedy is retargeting—mapping

human motions to robot kinematics [10], [11]—which is effective for teleoperation and data gathering but typically still requires reinforcement learning in simulation to attain dexterous proficiency, thereby introducing a sim-to-real gap and limiting cross-embodiment generalization. Recently, a more fundamental route is to learn manipulation structure from human hand data that robots can directly consume. For parallel-jaw grippers, PointPolicy [12] uses video-derived keypoints to supervise gripper control; however, such position-only cues under-specify dexterous-hand interaction. In this work, we therefore learn finger-specific affordances from human demonstrations—object-conditioned descriptors that specify, per finger, contactable regions to represent how dexterous hands should interact with objects.

### B. Object-centric Representation Learning

Much of object-centric grasping is tailored to parallel-jaw grippers, representing grasps by 2D/3D locations. Such position-only cues under-specify dexterous-hand interactions [13], [14]. In addition, a subset of dexterous hand approaches relies on template matching, built around exemplars specific to the object or the task, thus having limited generalizability to novel objects/tasks [15]. Contact-centric representations improve task relevance but require complex pipelines and costly data collection to obtain dexterous-hand contact regions [16]. More recently, interaction-driven approaches such as CMKA [17] learn interaction regions from web imagery, yet map object keypoints to wrist, index, and little-finger anchors, effectively producing a single grasp parameterized by three points and limiting performance to on-shelf settings. These limitations motivate per-finger contact representations rather than region- or point-only cues. We learn per-finger contact cues and, via depth-and-segmentation projection, map them onto object surfaces, to further derive precise tabletop grasps.

### C. Affordance Learning

However, most approaches localize coarse object regions (e.g., boxes or masks), which is insufficient for fine-grained, finger-specific guidance required by dexterous hands—motivating representations at the per-finger contact level.

## III. METHODS

We present a perception-to-optimization pipeline that learns *finger-specific affordances* from human demonstrations and uses them to synthesize executable dexterous grasps (Fig. 2). We extract semantically grounded hyperfeatures using a frozen text-to-image diffusion model [1] and decode them into five per-finger likelihood maps, which provide finger-wise contact priors on the object surface. We then formulate grasp synthesis as an *affordance-conditioned* optimization: the per-finger priors are incorporated as a finger-wise alignment term alongside force-closure and feasibility objectives, thereby coupling grasp pose generation with the learned affordance priors.

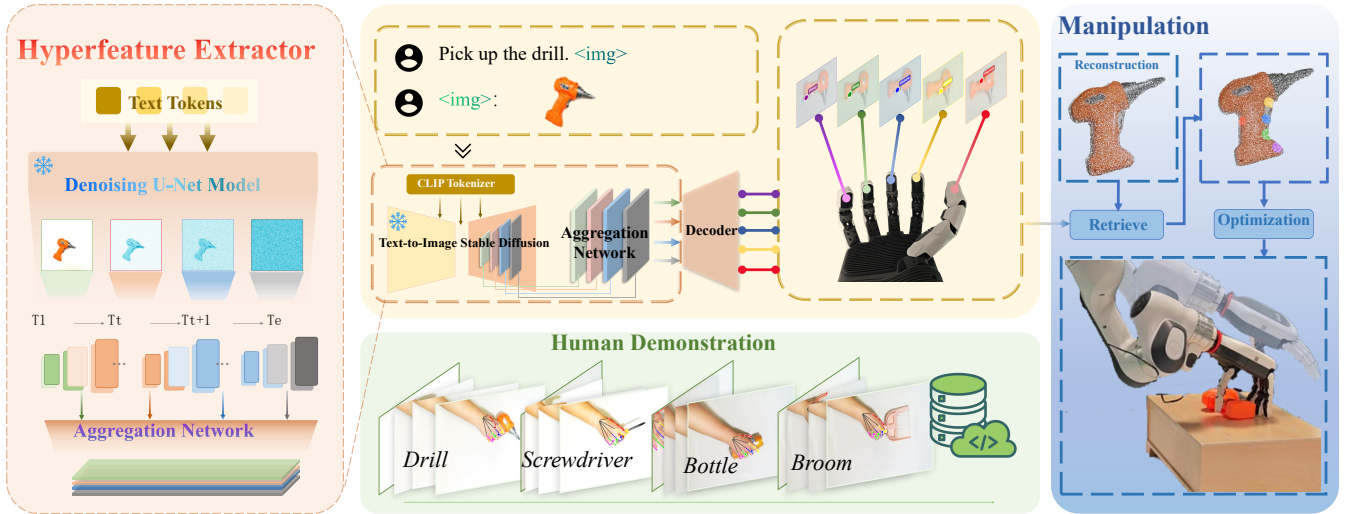


Fig. 2: **Pipeline overview.** (1) *Hyperfeature extraction*: A frozen text-to-image diffusion U-Net encodes the object image with text conditioning. Multi-timestep, multi-scale activations are aggregated into hyperfeatures  $A_g$ . (2) *Finger-specific affordance grounding*: An FPN-style decoder maps  $A_g$  to five per-finger likelihood maps  $\hat{H}$  supervised by fingertip labels from human demonstrations. (3) *Manipulation*: We reconstruct the object with SAM3+SAM3D, lift peaks of  $\hat{H}$  to 3D contacts, and augment GraspQP with a finger-specific affordance term to refine stable, human-intuitive grasps.

#### A. Data Collection

We construct a finger-wise contact affordance dataset from human demonstration videos using a custom data acquisition pipeline. For each recorded grasp sequence, we first automatically detect 2D hand keypoints with the RTMPose [18] hand pose estimator. We then identify (i) an *object-only* keyframe in which the target object is fully visible and no hand pixels are present, and (ii) the earliest *stable grasp* frame in which the human hand establishes clear contact with the object. This pair of frames form one training sample: the object-only frame provides a clean visual context of the object’s geometry and texture, while the grasp frame provides the supervisory signal for finger-specific contact localization.

On the image lattice  $\Omega = \{0, \dots, h-1\} \times \{0, \dots, w-1\}$ , each fingertip  $k$  with center  $\mu_k$  induces a Gaussian channel  $H_k(u) = \exp(-\|u - \mu_k\|_2^2 / (2\sigma^2))$  for  $u \in \Omega$ ; stacking yields a tensor  $H$  of shape  $5 \times h \times w$ . We set  $\sigma = \min(h, w)/64$  and train the predictor  $\hat{H}$  to regress  $H$  using MSE.

#### B. Finger-Specific Affordance Representation from Diffusion Models

1) *Feature synthesis and hyperfeature aggregation*: Empirical evidence that diffusion models generate precise hand-object grasp [8] scenarios indicates that Stable Diffusion [1] has already acquired the grasp-critical feature space, integrating holistic affordance semantics with nuanced image details via its generative learning process. Inspired by prior work [8], [19], we leverage the rich semantic grounding capability of large pretrained text-to-image diffusion models to localize finger-specific contact affordances on object images. Distinct from previous approaches, we jointly harvest both visual and textual affordance semantics from Stable Diffusion. Given an image-text pair  $(x_0, s)$ , we encode a latent  $z_0 = E(x_0)$  with the variational autoencoder (VAE) and

follow the standard *latent* forward noising process

$$z_t = \sqrt{\bar{\alpha}_t} z_0 + \sqrt{1 - \bar{\alpha}_t} \epsilon, \quad \epsilon \sim \mathcal{N}(0, I), \quad (1)$$

where  $\bar{\alpha}_t = \prod_{\tau=1}^t \alpha_\tau$  as defined in [1]. We keep the text encoder  $T(\cdot)$  frozen and obtain token embeddings  $c = T(s)$ . For computational reasons, we run the diffusion network for  $T$  timesteps but only select a subset  $\mathcal{S}$  with  $|\mathcal{S}| = S$  for feature aggregation. Feeding  $(z_t, t, c)$  into a frozen diffusion U-Net yields multi-scale activations:

$$\{A_{v,1}^{(t)}, A_{v,2}^{(t)}, \dots, A_{v,L}^{(t)}\}, \quad t \in \mathcal{S},$$

Here,  $A_{v,\ell}^{(t)} \in \mathbb{R}^{B \times C_\ell \times H_\ell \times W_\ell}$  denotes the feature map from the  $\ell$ -th U-Net block at timestep  $t$ .

To summarize complementary semantics across scales and timesteps, we attach lightweight bottlenecks  $\{b_\ell\}_{\ell=1}^L$  (shared across timesteps) and learn mixing coefficients  $\{w_{\ell,t}\}_{\ell=1,t \in \mathcal{S}}^L$  to produce a global affordance descriptor:

$$A_g = \sum_{t \in \mathcal{S}} \sum_{\ell=1}^L w_{\ell,t} b_\ell(A_{v,\ell}^{(t)}). \quad (2)$$

In practice, each  $b_\ell$  is a  $1 \times 1$  convolution followed by global average pooling to a fixed  $d$ -dimensional vector. We parameterize  $\tilde{w}_{\ell,t}$  freely and apply a softmax over all  $(\ell, t)$ .

2) *Finger-Specific Affordance Heatmap Prediction*: To enhance the fine-grained finger-specific affordance grounding ability while preserving high-level semantic discrimination and recovering spatial details, we proposed a feature pyramid network (FPN)-style decoder, which progressively upsamples  $A_g$  while injecting lateral features from shallower resolutions, producing a dense fused feature map suitable for contact prediction.

Given the dense hyperfeature  $A_g \in \mathbb{R}^{B \times C \times h \times w}$ , we decode it with three lateral  $1 \times 1$  projections  $\{\phi_r\}_{r=3}^1$  (to channels

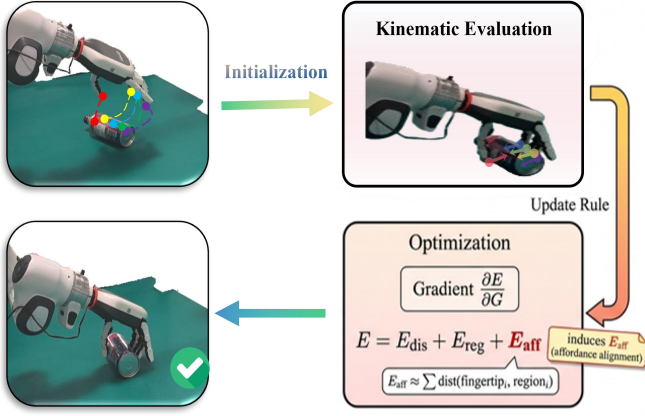


Fig. 3: Finger-Specific Affordance Field (FSAF) regions on the object induce an affordance-alignment term  $E_{\text{aff}}$ .

$c_r \in \{256, 128, 64\}$ ) and a top-down pathway. Let target sizes  $s_3=(h, w)$ ,  $s_2=(2h, 2w)$ ,  $s_1=(H_{\text{out}}, W_{\text{out}})$ ,  $U_s$  be bilinear upsampling to size  $s$ ,  $\tau_r$  a  $1 \times 1$  adapter, and  $\psi_r$  a  $3 \times 3$  smoothing conv with nonlinearity. With  $F_4 \equiv 0$ , we compute

$$F_r = \psi_r \left( U_{s_r} (\tau_r(F_{r+1})) + U_{s_r} (\phi_r(A_g)) \right), \quad r = 3, 2, 1, \quad (3)$$

and obtain the per-finger heatmaps by a final  $3 \times 3$  projection

$$\hat{H} = \kappa(F_1) \in \mathbb{R}^{B \times K \times H_{\text{out}} \times W_{\text{out}}}, \quad K = 5. \quad (4)$$

We optimize a mean squared error (MSE) loss over all fingers and pixels:

$$\mathcal{L}_{\text{MSE}} = \frac{1}{5|\Omega|} \sum_{k=1}^5 \sum_{u \in \Omega} (\hat{H}_k(u) - H_k(u))^2. \quad (5)$$

### C. Finger-Specific Affordance Matching for Dexterous Grasping

#### Object Reconstruction and Affordance Grounding.

We first segment the target object with SAM3 [20] and back-project the masked RGB-D depth into a partial object point cloud using the camera intrinsics. We then apply a reconstruction pipeline based on SAM3D [21] to obtain a posed object surface, and refine the estimated pose via ICP. The resulting object-to-camera transform is denoted as  $\mathbf{T}_{\text{obj} \rightarrow \text{cam}} \in SE(3)$ .

Using the finger-specific affordances derived in Section III-B, we re-project the object’s point cloud onto the image plane. For each predicted finger keypoint, we identify the nearest  $N$  point-cloud projections on the image, forming a set of robust fingertip contact candidates.

**Grasp Refinement and Integration of Finger-Specific Affordances.** Our grasp refinement module is inspired by GraspQP [22] and we introduce key innovations by refining this approach to account for finger-specific affordance cues, allowing for more precise and targeted grasp synthesis.

We minimize the following energy function to ensure the grasp is physically stable and meanwhile, aligned with the affordance regions of each finger:

$$E = E_{\text{fc}} + w_{\text{dis}} E_{\text{dis}} + w_{\text{reg}} E_{\text{reg}} + w_{\text{aff}} E_{\text{aff}}, \quad (6)$$

where  $E_{\text{fc}}$  is a force-closure term from GraspQP that optimizes contact force distributions to balance external wrenches under Coulomb friction. The term  $E_{\text{dis}}$  penalizes the distance between active contact points  $\mathcal{C}'$  and the object surface, ensuring proper contact placement, while  $E_{\text{reg}}$  consists of regularization terms designed to prevent hand-object penetration, joint-limit violations, and self-penetration.

We incorporate Finger-Specific Affordance Fields (FSAF) into grasp refinement as a finger-conditioned geometric prior. **Affordance prior in the objective.** Concretely, to instantiate the affordance regularizer in the refinement objective defined above, we add the following contact-to-region alignment term:

$$E_{\text{aff}} = \frac{1}{|\mathcal{C}'|} \sum_{j \in \mathcal{C}'} \min_{q \in S_g(j)} \|c_j - q\|_2^2, \quad (7)$$

where  $\mathcal{C}'$  denotes the set of contact points optimized during refinement, and  $g(j)$  maps each contact  $c_j$  to its corresponding finger-specific affordance region  $S_{g(j)}$ . Minimizing the full objective thus encourages contacts to stay on their predicted regions while the remaining terms enforce physical feasibility.

**Initialization (warm start).** We warm-start the refinement solver with an affordance-consistent contact layout: for each finger  $i$ , we initialize its fingertip contact  $c_i$  near  $S_i$  by enforcing  $\text{dist}(c_i, S_i) \leq \delta$  with  $\delta = 3$  cm. This narrows the search to role-consistent configurations and reduces sensitivity to local minima.

**Execution.** After optimizing the objective to obtain the refined grasp posture, we execute a three-phase motion plan—*approach*, *close*, and *hold*—to realize smooth finger trajectories and stable contact establishment. We evaluate grasp quality and task performance in Sec. IV-C.

## IV. EXPERIMENTS

In this section, we conduct comprehensive experiments to validate our method from three complementary perspectives: **RQ1:** Does the proposed finger-specific grasp representation outperform prior keypoint/affordance grounding, and does leveraging vision-language priors from Stable Diffusion model yield gains over discriminative backbones?

**RQ2:** Does the method improve grasp stability and produce more human-intuitive contact placements on seen and unseen objects, especially for categories with weak part cues?

**RQ3:** Does the learned finger-specific affordance representation transfer across dexterous hands with minimal adaptation?

### A. Experimental Setup

**Dataset:** We collect 130 *finger-specific* human grasp demonstrations over 13 everyday objects (10 per object; e.g., banana, screwdriver, bottle). For evaluation, we test on seven *unseen* objects that include both (i) new instances of previously seen categories and (ii) entirely novel categories (e.g., wrench, hammer).

**Implementation Details:** We train for 4,000 steps with batch size 2 on a single NVIDIA H100 GPU using AdamW (initial learning rate  $10^{-3}$  with cosine decay). Raw RGB

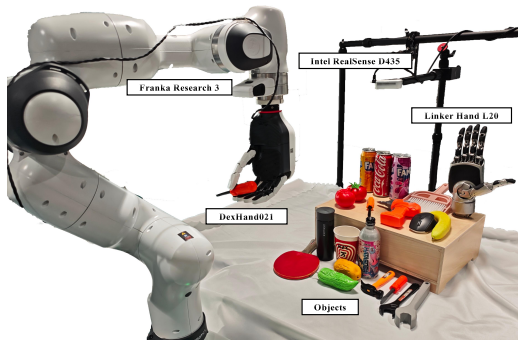


Fig. 4: Robotic arm and dexterous-hand experimental platform used in our study.

frames are resized to  $640 \times 320$  with letterboxing when necessary to preserve aspect ratio, and pixel intensities are normalized to  $[0, 1]$ . Predicted and ground-truth finger heatmaps are uniformly rescaled to  $448 \times 448$  following saliency-grounding conventions, and each per-finger heatmap is re-normalized to integrate to 1. All results are averaged over 3 random seeds. The robotic arm–dexterous-hand platform is shown in Fig. 4; the real-world setup comprises two dexterous hands (DexHand021 and Linker Hand L20), a Franka arm, and a RealSense 435 camera.

**Evaluation Metrics:** For finger-specific affordance grounding, We report KLD, SIM, and NSS [23], **following CMKA [17] for metric computation:**

- **KLD** (lower is better): Kullback–Leibler divergence between predicted and ground-truth heatmaps.
- **SIM** (higher is better): Normalized histogram intersection (similarity).
- **NSS** (higher is better): Normalized Scanpath Saliency; per finger we sample the annotated keypoint location as a fixation.

For Dexterous grasping, we follow the definitions of metrics provided in [4] and [5]: **Grasping Success Rate (Suc. R.)**: A grasp is considered successful if the object can be lifted above 0.1 m and held stable longer than 3 seconds. Here, grasping specifically refers to grasping based on manipulation affordances.

### B. Results of Finger-Specific Affordance Grounding

Because there is no prior work that directly couples vision-language models with fine-grained, finger-specific affordance keypoints, we select the closest approach as the baseline. CMKA [17] leverages exocentric (third-person) interaction images as input, applies SAM [24] for multi-scale object segmentation, and then performs clustering over the segmentation-driven feature hierarchy to learn object affordance keypoints. To ensure fairness, we train CMKA [17] using the exocentric interaction images from **our dataset**, keeping all other hyperparameters unchanged. For metric computation, we follow a procedure consistent with CMKA: the predicted keypoints are first rescaled to the original image resolution, then converted into heatmaps by placing Gaussian kernels centered at each keypoint. To validate the necessity of large-scale generative models in our framework,

TABLE I: Comparison and ablation on the finger-specific affordance grounding benchmark. Best results in **bold**. ( $\uparrow$ / $\downarrow$  denote higher/lower is better.)

Model / Variant	KLD( $\downarrow$ )	SIM( $\uparrow$ )	NSS( $\uparrow$ )
CMKA [17]	11.184	0.177	1.861
Ours (CLIP)	6.690	0.355	3.815
Ours (DINO)	3.301	0.473	5.016
Ours (SD)	<b>2.491</b>	<b>0.551</b>	<b>5.518</b>

We ablate feature extractors by replacing SD hyperfeatures with CLIP [25] and DINO [26]

Table I shows that CMKA underperforms on finger-specific affordance grounding: its segmentation-driven hierarchy is brittle when objects lack distinctive, part-aligned visual regions. Fig. 5 (seen vs. unseen) illustrates typical failures, where predictions collapse toward object centroids or spill across boundaries, yielding contacts that miss functional parts. In contrast, our method improves all three metrics (lower KLD, higher SIM/NSS), indicating sharper, part-aligned localization rather than generic centers or silhouette edges.

Holding data, labels, losses, and the training schedule fixed while varying only the feature extractor, we isolate the contribution of diffusion hyperfeatures. Compared with DINO/CLIP, **KLD** increases by  $1.33\times/2.69\times$ , while **SIM** drops by  $14.2\%/35.6\%$  and **NSS** by  $9.1\%/30.9\%$ . Qualitatively, DINO features more often merge adjacent fingers and produce broader activations with boundary spill-over; on unseen elongated tools, they also bias toward visually salient parts rather than human-intuitive grasp regions. Diffusion hyperfeatures consistently suppress three dominant errors—centroid collapse, boundary spill-over, and fingertip swapping—supporting **RQ1** that they are critical for precise per-finger affordance localization.

### C. Functional Affordance Grasping with High-DOF Hands

Our evaluation targets *on-table*, affordance-driven dexterous grasping with finger-specific contacts and human-consistent grasp sites. Existing simulation-trained policies [2] optimize for success in simplified settings and cannot select grasp sites following human conventions (e.g., grasping a hammer by its head). To assess alignment with human grasp choices within our setting, we include two point-cloud-based imitation learning policies (Diffusion Policy 3D [27] and ACT-3D [28]) trained from our teleoperated demonstrations (30 trajectories). We also compare to CMKA, representing a recent affordance-based dexterous grasping approach. We evaluate CMKA strictly under its original, unmodified pipeline: we directly use the three keypoints predicted by CMKA, lift them to 3D, assign them to the functional finger, little finger, and wrist, and then execute the method’s fixed grasp execution strategy. We additionally compare with GrainGrasp [29], a representative fine-grained contact-guided grasp synthesis method, by adapting its contact-guided refinement stage to our robotic hand embodiment

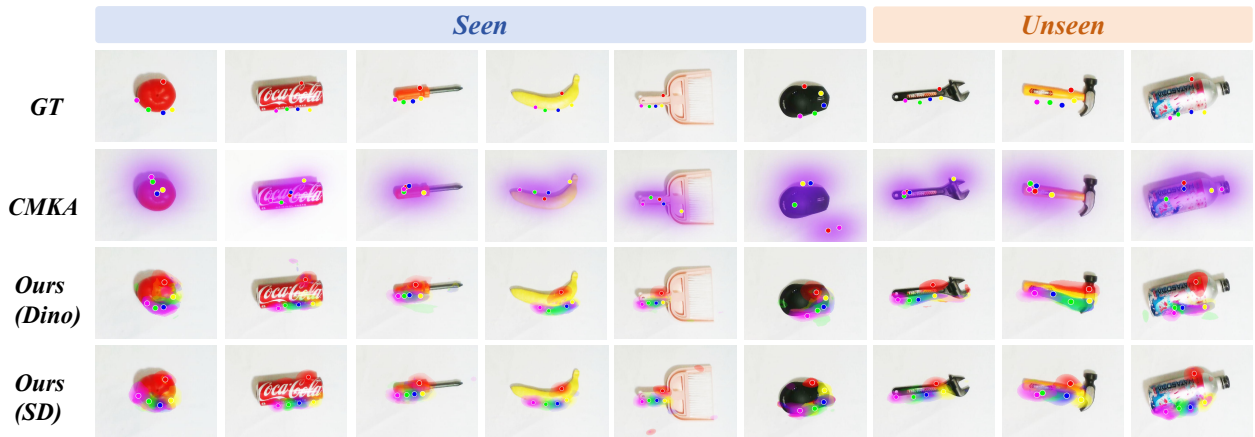


Fig. 5: **Qualitative comparison of finger-specific affordance grounding.** Left: *Seen* objects; Right: *Unseen* objects. Rows show CMKA, Ours (DINO features), and Ours (Stable Diffusion). Overlays visualize five per-finger likelihood maps; colored dots indicate annotated fingertip contacts. The diffusion-based variant produces sharper, finger-disentangled hotspots aligned with functional parts and preserves localization quality on unseen tools. CMKA produces keypoints directly and a single-channel heatmap is generated via post-processing following CMKA, thus its overlays are rendered in a single purple color, whereas our method outputs five-channel heatmaps rendered with five distinct colors.

and evaluating it under the same perception and execution pipeline for real-robot success-rate comparison.

Fig. 6 presents qualitative grasp predictions on the Linker Hand L20 for GrainGrasp, GraspQP, and our method. Our approach consistently produces human-intuitive grasp poses: guided by finger-specific affordances, the fingertips align tightly with the predicted graspable regions, yielding contact layouts that match the functional geometry of each object. In contrast, GraspQP with random initialization performs markedly worse, often converging to non-human-like poses (e.g., on the *screwdriver*), missing the intended grasp regions, and occasionally producing degenerate configurations with overlapping fingers. GraspQP\* (GraspQP with the same region-conditioned initialization as our method) can sometimes achieve similarly reasonable grasps on *bottle*, *tomato*, and *screwdriver*, indicating that a strong warm start already alleviates some local-minima failures; however, it still fails on the *banana* and converges to visually implausible configurations on the *drill*, suggesting that initialization alone is insufficient to enforce affordance-consistent, finger-wise contact placement. It’s also noteworthy that GrainGrasp fails to generate meaningful grasps across these objects, as it is tailored to MANO-scale human hands and its contact representation and kinematic assumptions do not transfer well to high-DOF robotic hands.

As shown in Tab. II, the conventional imitation-learning baselines (ACT-3D AND Diffusion Policy 3D) tend to reproduce trajectories close to demonstrations: as object morphology varies, they do not proactively adapt their strategy, leading to significantly degraded performance both on seen objects with poses absent from the training data and on unseen objects. GrainGrasp, while leveraging contact cues extracted from human-hand demonstrations, is hindered by the lack of cross-demonstration consistency in the resulting contact patterns, which makes contact-conditioned pose syn-

TABLE II: Performance comparison across different methods on common objects and tools manipulation tasks. Each cell reports  $N=20$  trials per object (S = seen, U = unseen). We additionally report cross-embodiment transfer of our method on two dexterous hands.

Model	Common Objects (%)			Tools (%)	
	Bottle (S/U)	Banana	Tomato	Screwdriver	Drill
ACT-3D [28]	30/25	30	50	30	40
Diffusion Policy 3D [27]	40/40	50	45	0	30
GrainGrasp [29]	0/0	0	0	0	0
CMKA [17]	30/20	20	0	0	60
Ours (DexHand021)	<b>100/85</b>	<b>85</b>	<b>90</b>	<b>60</b>	<b>70</b>
Ours (Linker Hand L20)	<b>100/80</b>	<b>90</b>	<b>100</b>	<b>70</b>	<b>90</b>

thesis brittle under distribution shift. Moreover, the method is evaluated only in simulation and its contact-to-grasp stage does not explicitly enforce real-robot grasp feasibility (e.g., force-closure and frictional stability under hardware and contact uncertainties); consequently, it attains near-zero success in our real-robot protocol (Tab. II), underscoring the practical difficulty of sim-to-real transfer for contact-guided grasp synthesis. Meanwhile, CMKA’s performance is limited by the layered segmentation output of SAM; as discussed in Section II-B, for objects that lack salient part delineation such as tomatoes and bananas, it often fails to predict correct grasp locations. Moreover, because it executes a preprogrammed grasp approaching motion, the fingers collide with the table surface when attempting to grasp low-profile objects such as bananas and screwdrivers, thus preventing successful task completion.

Fig. 8 plots energy over the full refinement, including multiple resets. Although our objective augments the original GraspQP formulation with an additional affordance alignment term  $E_{\text{aff}}$ , it consistently converges faster than GraspQP\* after *each* reset and reaches a lower final energy

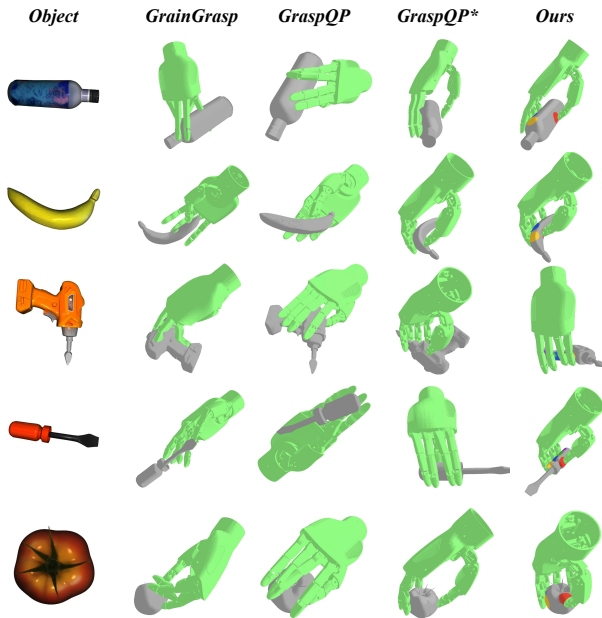


Fig. 6: **Qualitative grasp visualization.** We visualize predicted grasps on five objects (bottle, banana, drill, screwdriver, and tomato). From left to right, we compare GrainGrasp, GraspQP with random initialization, GraspQP\* (GraspQP initialized in the same way as ours), and our method. In the last column, the colored surface regions on the object mesh indicate our predicted finger-specific affordances.

overall. We attribute this improvement to the fact that  $E_{\text{aff}}$  provides a dense, region-consistent geometric signal that pulls finger contacts toward the predicted graspable surface regions, thereby shrinking the effective search space and steering the optimizer away from poor local minima. In practice, this contact-level guidance also indirectly benefits the force-closure term  $E_{\text{fc}}$ : by promoting more plausible and better-situated contacts, the solver more readily finds feasible contact force distributions that balance external wrenches, resulting in higher-quality grasps at convergence.

a) *Cross-Embodiment Evaluation.*: Beyond the Dex-Hand021 used in the preceding experiments, we further test the same pipeline on another dexterous hand embodiment (Linker Hand L20). We transfer the pipeline from Dex-Hand021 (12+5 DOFs) to Linker Hand L20 (16+5 DOFs); perception and affordance inference remain unchanged. As shown in Tab. II, grasp success remains statistically unchanged across embodiments. This invariance indicates that the proposed finger-specific affordance representation and geometry-aligned waypoint construction decouple grasp semantics from hand morphology, enabling deployment without hand-specific retraining.

## V. CONCLUSION AND FUTURE WORK

We propose *Finger-Specific Affordance Grounding* (FSAG), which learns per-finger contact affordances from a small set of human demonstrations. Our key idea is to repurpose a frozen text-to-image diffusion model as a

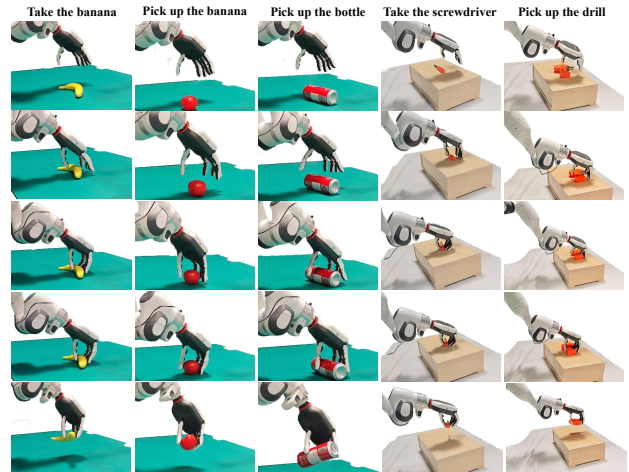


Fig. 7: **Affordance-driven dexterous grasping in the real world.** Representative rollouts on everyday objects and tools; columns denote tasks (banana, bottle, tomato, screwdriver, drill).

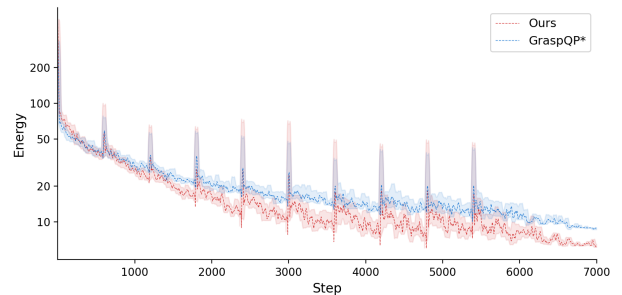


Fig. 8: **Energy convergence over the full optimization.** Energy vs. optimization step throughout the entire refinement process. The blue curve corresponds to GraspQP\* (GraspQP with the same initialization as our method), while the red curve denotes our method.

semantic backbone and train a lightweight decoder to predict five finger-conditioned likelihood maps, bridging high-level interaction priors with fine-grained contact localization. We lift the predicted per-finger affordance maps to object-surface regions and *couple* them with physically grounded grasp refinement, jointly optimizing contact feasibility and finger-region consistency to produce stable, human-intuitive grasps. Empirically, our approach substantially outperforms contemporary methods on both affordance localization accuracy and human-intuitive grasping success rate.

## REFERENCES

- [1] R. Rombach, A. Blattmann, D. Lorenz, P. Esser, and B. Ommer, “High-resolution image synthesis with latent diffusion models,” in *Proceedings of the IEEE/CVF conference on computer vision and pattern recognition*, 2022, pp. 10 684–10 695.
- [2] Y. Xu, W. Wan, J. Zhang, H. Liu, Z. Shan, H. Shen, R. Wang, H. Geng, Y. Weng, J. Chen *et al.*, “Unidexgrasp: Universal robotic dexterous grasping via learning diverse proposal generation and goal-conditioned policy,” in *Proceedings of the IEEE/CVF Conference on Computer Vision and Pattern Recognition*, 2023, pp. 4737–4746.

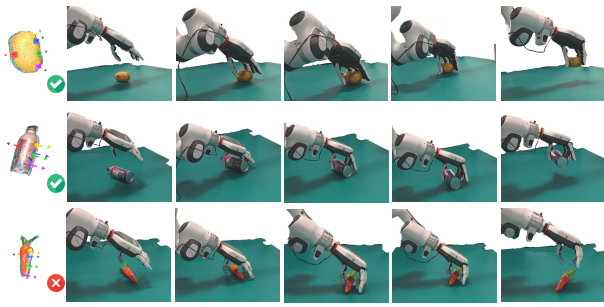


Fig. 9: Zero-shot generalization on unseen objects

- [3] R. Wang, J. Zhang, J. Chen, Y. Xu, P. Li, T. Liu, and H. Wang, “Dexgraspnet: A large-scale robotic dexterous grasp dataset for general objects based on simulation,” *arXiv preprint arXiv:2210.02697*, 2022.
- [4] H.-S. Fang, H. Yan, Z. Tang, H. Fang, C. Wang, and C. Lu, “Anydex-grasp: General dexterous grasping for different hands with human-level learning efficiency,” *arXiv preprint arXiv:2502.16420*, 2025.
- [5] H. Luo, W. Zhai, J. Zhang, Y. Cao, and D. Tao, “Learning visual affordance grounding from demonstration videos,” *IEEE Transactions on Neural Networks and Learning Systems*, 2023.
- [6] —, “Learning affordance grounding from exocentric images,” in *Proceedings of the IEEE/CVF conference on computer vision and pattern recognition*, 2022, pp. 2252–2261.
- [7] A. Dosovitskiy, L. Beyer, A. Kolesnikov, D. Weissenborn, X. Zhai, T. Unterthiner, M. Dehghani, M. Minderer, G. Heigold, S. Gelly, J. Uszkoreit, and N. Houlsby, “An image is worth 16x16 words: Transformers for image recognition at scale,” in *International Conference on Learning Representations*, 2021. [Online]. Available: <https://openreview.net/forum?id=YicbFdNTTy>
- [8] J. Yang, B. Li, F. Yang, A. Zeng, L. Zhang, and R. Zhang, “Boosting human-object interaction detection with text-to-image diffusion model,” *arXiv preprint arXiv:2305.12252*, 2023.
- [9] J. Ren, P. Sundaresan, D. Sadigh, S. Choudhury, and J. Bohg, “Motion tracks: A unified representation for human-robot transfer in few-shot imitation learning,” *arXiv preprint arXiv:2501.06994*, 2025.
- [10] S. Zhao, X. Zhu, Y. Chen, C. Li, X. Zhang, M. Ding, and M. Tomizuka, “Dexh2r: Task-oriented dexterous manipulation from human to robots,” *arXiv preprint arXiv:2411.04428*, 2024.
- [11] K. Li, P. Li, T. Liu, Y. Li, and S. Huang, “Maniptrans: Efficient dexterous bimanual manipulation transfer via residual learning,” in *Proceedings of the Computer Vision and Pattern Recognition Conference*, 2025, pp. 6991–7003.
- [12] S. Haldar and L. Pinto, “Point policy: Unifying observations and actions with key points for robot manipulation,” *arXiv preprint arXiv:2502.20391*, 2025.
- [13] M. K. Srirama, S. Dasari, S. Bahl, and A. Gupta, “Hrp: Human affordances for robotic pre-training,” *arXiv preprint arXiv:2407.18911*, 2024.
- [14] W. Dong, D. Huang, J. Liu, C. Tang, and H. Zhang, “Rtagrasp: Learning task-oriented grasping from human videos via retrieval, transfer, and alignment,” in *2025 IEEE International Conference on Robotics and Automation (ICRA)*. IEEE, 2025, pp. 1–7.
- [15] M. Kokic, D. Kragic, and J. Bohg, “Learning task-oriented grasping from human activity datasets,” *IEEE Robotics and Automation Letters*, vol. 5, no. 2, pp. 3352–3359, 2020.
- [16] L. Yang, K. Li, X. Zhan, F. Wu, A. Xu, L. Liu, and C. Lu, “Oakink: A large-scale knowledge repository for understanding hand-object interaction,” in *Proceedings of the IEEE/CVF conference on computer vision and pattern recognition*, 2022, pp. 20953–20962.
- [17] F. Yang, D. Luo, W. Chen, J. Lin, J. Cai, K. Yang, Z. Li, and Y. Wang, “Multi-keypoint affordance representation for functional dexterous grasping,” *arXiv preprint arXiv:2502.20018*, 2025.
- [18] T. Jiang, P. Lu, L. Zhang, N. Ma, R. Han, C. Lyu, Y. Li, and K. Chen, “Rtmpose: Real-time multi-person pose estimation based on mmpose,” *CoRR*, 2023.
- [19] G. Luo, L. Dunlap, D. H. Park, A. Holynski, and T. Darrell, “Diffusion hyperfeatures: Searching through time and space for semantic correspondence,” *Advances in Neural Information Processing Systems*, vol. 36, pp. 47500–47510, 2023.
- [20] N. Carion, L. Gustafson, Y.-T. Hu, S. Debnath, R. Hu, D. Suris, C. Ryali, K. V. Alwala, H. Khedr, A. Huang, J. Lei, T. Ma, B. Guo, A. Kalla, M. Marks, J. Greer, M. Wang, P. Sun, R. Rädle, T. Afouras, E. Mavroudi, K. Xu, T.-H. Wu, Y. Zhou, L. Momeni, R. Hazra, S. Ding, S. Vaze, F. Porcher, F. Li, S. Li, A. Kamath, H. K. Cheng, P. Dollár, N. Ravi, K. Saenko, P. Zhang, and C. Feichtenhofer, “Sam 3: Segment anything with concepts,” 2025. [Online]. Available: <https://arxiv.org/abs/2511.16719>
- [21] S. D. Team, X. Chen, F.-J. Chu, P. Gleize, K. J. Liang, A. Sax, H. Tang, W. Wang, M. Guo, T. Hardin, X. Li, A. Lin, J. Liu, Z. Ma, A. Sagar, B. Song, X. Wang, J. Yang, B. Zhang, P. Dollár, G. Gkioxari, M. Feiszli, and J. Malik, “Sam 3d: 3dfy anything in images,” 2025. [Online]. Available: <https://arxiv.org/abs/2511.16624>
- [22] R. Zurbrügg, A. Cramariuc, and M. Hutter, “Grasppq: Differentiable optimization of force closure for diverse and robust dexterous grasping,” in *Conference on Robot Learning (CoRL)*, 2025. [Online]. Available: <https://grasppq.github.io/>
- [23] Z. Bylinskii, T. Judd, A. Oliva, A. Torralba, and F. Durand, “What do different evaluation metrics tell us about saliency models?” *IEEE transactions on pattern analysis and machine intelligence*, vol. 41, no. 3, pp. 740–757, 2018.
- [24] A. Kirillov, E. Mintun, N. Ravi, H. Mao, C. Rolland, L. Gustafson, T. Xiao, S. Whitehead, A. C. Berg, W.-Y. Lo *et al.*, “Segment anything,” in *Proceedings of the IEEE/CVF international conference on computer vision*, 2023, pp. 4015–4026.
- [25] A. Radford, J. W. Kim, C. Hallacy, A. Ramesh, G. Goh, S. Agarwal, G. Sastry, A. Askell, P. Mishkin, J. Clark *et al.*, “Learning transferable visual models from natural language supervision,” in *International conference on machine learning*. Pmlr, 2021, pp. 8748–8763.
- [26] M. Caron, H. Touvron, I. Misra, H. Jégou, J. Mairal, P. Bojanowski, and A. Joulin, “Emerging properties in self-supervised vision transformers,” in *Proceedings of the IEEE/CVF international conference on computer vision*, 2021, pp. 9650–9660.
- [27] Y. Ze, G. Zhang, K. Zhang, C. Hu, M. Wang, and H. Xu, “3d diffusion policy: Generalizable visuomotor policy learning via simple 3d representations,” in *ICRA 2024 Workshop on 3D Visual Representations for Robot Manipulation*.
- [28] T. Gervet, Z. Xian, N. Gkanatsios, and K. Fragkiadaki, “Act3d: 3d feature field transformers for multi-task robotic manipulation,” in *7th Annual Conference on Robot Learning*, 2023. [Online]. Available: <https://openreview.net/forum?id=HFJuX1uqs>
- [29] F. Zhao, D. Tsetsrukou, and Q. Liu, “Graingrasp: Dexterous grasp generation with fine-grained contact guidance,” in *2024 IEEE International Conference on Robotics and Automation (ICRA)*, 2024, pp. 6470–6476.